metals

MDPI

Article

Impact of Remelting on ZnAl4Cu3 Alloy with Addition of Cd on Selected Technological and Mechanical Properties

Dana Bolibruchová, Marek Bruna and Marek Matejka *

Department of Technological Engineering, Faculty of Mechanical Engineering, University of Zilina, Univerzitná 8215/1, 010 26 Žilina, Slovakia; danka.bolibruchova@fstroj.uniza.sk (D.B.); marek.bruna@fstroj.uniza.sk (M.B.)

* Correspondence: marek.matejka@fstroj.uniza.sk; Tel.: +421-41-513-2772

Abstract: One of the main objectives in order to increase economic efficiency in foundries is to determine the ratio of the scrap material which can be used in the further manufacture. This factor is important for determining the final prices of products and their competitiveness, given that the prices of zinc on world markets have increased significantly in the recent years. This article deals with the possibilities of remelting the zinc foundry alloy ZnAl4Cu3 and also evaluates the effect of cadmium on selected properties. The main goal is to provide a comprehensive view of the influence of these two factors on selected mechanical properties, casting properties, and microstructure. An important part of the research is to point out the combined influence of given factors. The results of experiments confirmed that an addition of 3 wt.% of Cd has a significant impact on technological and mechanical properties. Fluidity values compared to the Cd-free alloy increased by 22.4%. In terms of mechanical properties, the influence of Cd on the tensile strength was most visible, with a decrease in average by 25 MPa.

Keywords: remelting; Tekcast; zinc alloy; microstructure; mechanical properties

check for updates

Citation: Bolibruchová, D.; Bruna, M.; Matejka, M. Impact of Remelting on ZnAl4Cu3 Alloy with Addition of Cd on Selected Technological and Mechanical Properties. *Metals* **2022**, *12*, 1180. https://doi.org/10.3390/met12071180

Academic Editors: Crystopher Cardoso de Brito and Paolo Ferro

Received: 9 June 2022
Accepted: 8 July 2022
Published: 11 July 2022

Publisher's Note: MDPI stays neutral with regard to jurisdictional claims in published maps and institutional affiliations.

Copyright: © 2022 by the authors. Licensee MDPI, Basel, Switzerland. This article is an open access article distributed under the terms and conditions of the Creative Commons Attribution (CC BY) license (https://creativecommons.org/licenses/by/4.0/).

1. Introduction

In zinc alloy foundries for centrifugal casting into silicone molds (Tekcast method), only the primary alloy is used for the production of castings. The casting design and number of castings placed in the mold determine the ratio between the castings volumes and the gating system volume. The gating system volume has a constant value when using the centrifugal casting method. That is why a large amount of scrap is created during the production of small castings. The role of recycling in the metallurgical sector has always been crucial and predominant and has had a major impact not only on the global economy and energy consumption, but also on the ecological environment and human life [1].

In terms of energy consumption, secondary or recycled zinc consumes less than 10% of the energy required to produce primary zinc. By using more recycled metal, a huge amount of air pollution generated by power plants can be eliminated. Research by Hsien Hui Khoo [2] displays the Final Weighted Scores (indirect emissions) for the primary-to-recycled metal mixes of 100% primary zinc, 50–50% primary-to-recycled zinc, 40–60% primary-to-recycled zinc, and finally 100% recycled zinc. From the first (100% primary metal) to the second graph and third graph (metal mixes), up to about a 50% reduction in power-plant emissions can be reduced. Moreover, when 100% recycled zinc is used, the overall environmental load drops by 90%. However, due to the adverse effects on material characteristics and product quality, it is impossible to use 100% recycled zinc for casting. However, efforts to increase the content of recycled zinc, from its present value in castings, should continue [2].

One of the main objectives in order to increase economic efficiency in foundries is to determine the ratio of the scrap material which can be used in the further manufacture

(after the recycling process). This factor is important for determining the final prices of products and their competitiveness, given that the prices of zinc on world markets have increased significantly in the recent years [3].

At present, zinc is the fourth most widely used metal in the world, after iron, aluminum, and copper. The recycling and production of secondary zinc alloys accounts for 30% of the global zinc consumption. The level of recycling is increasing in line with advances in zinc production and zinc recycling technologies [4–6]. Zinc is most often used as a coating element or as an alloying element. The production of zinc alloys accounts for 15% of its consumption [7,8]. Zn-Al alloys are classified on the basis of chemical composition: hypereutectic zinc alloys (over 5.1 wt.% Al), eutectic zinc alloys (5.1 wt.% Al), and hypoeutectic zinc alloys (less than 5.1 wt.% Al) [9]. Hypoeutectic alloys are known as Zamak alloys and make up the majority of the zinc alloys produced. The ZAMAK 2 alloy has the best mechanical properties of Zamak alloys in terms of tensile strength, creep resistance, and hardness. It is a commercial material that is widely used for the production of mechanically stressed components [10].

The presence of Cu (3% wt.%) plays an important role in the alloy itself [11,12]. Cu improves mechanical properties by forming CuZn4 precipitates; however, a Cu content greater than 1.25 wt.% causes undesirable dimensional instability. By forming the intermetallic phase CuZn4, the copper content in the matrix precipitates, and this intermetallic phase crystallizes at the eutectic temperature (377 °C) as a result of the following reaction: $L \rightarrow \alpha + \eta + E$. Moreover, at the temperature 268 °C, the following reactions occur: $\alpha + E \rightarrow \eta + T'$, forming a stable phase Al4Cu3Zn [13,14]. These phase formations reduce the solid solution strengthening effect. The hardness of the alloy increases with the formation of CuZn4 particles. These particles are harder than the matrix, but there is an increasing tendency to crack [15–17]. The formation of these Cu-rich intermetallic phases leads to a reduction in Cu content in primary η (Zn-rich phase in hexagonal morphology), which causes a decrease in strength due to reduced solid solution solidification [16,18].

Cadmium in zinc alloys is classified as an unwanted contaminant in terms of its negative effects on the human organism. Under European conditions, ZAMAK alloys with Cd are not allowed. On other continents, its usage is allowed, claiming that Zn with Cd creates eutectics that do not cause harmful effects on the human body. On the other hand, it can improve the fluidity, especially in castings with complicated shapes [19]. Cadmium as an alloying element in zinc alloys is currently not described at all, and there are almost no scientific articles dealing with this issue. Pola states that the presence of Cd in a zinc alloy improves the wear resistance, especially at high loads (30–45 N) [8]. On the other hand, Cd causes inter-granular corrosion in Zn-Al alloys and reduces the physical properties of the alloy [20].

The aim of this paper is to analyze the actual effect of multiple remelting for the "pure" ZAMAK 2 alloy and the ZAMAK 2 alloy with cadmium addition. Another objective is to evaluate how multiple remeltings or the addition of Cd affects the casting and mechanical properties with connection to the microstructure of experimental alloys. Scientific studies focusing on a given alloy and Cd as the alloying element are very limited, so deeper research could help to increase its applications in practice.

2. Experimental Material and Methodology

2.1. Alloy and Casting Parameters

The ZnAl4Cu3 (ZAMAK2) alloy was used to perform the experimental work. This alloy is designed for HPDC and centrifugal casting into silicone molds. ZnAl4Cu3 is a hypo-eutectic alloy that has a narrow solidification interval and has good casting properties. This experimental alloy is characterized by a high-quality surface, which allows further surface treatment (for example by galvanic plating), with minimal requirements for further machining. The suitability of this alloy for pressure and centrifugal casting methods consists in the rapid crystallization in the mold. The chemical composition of the reference

alloy (after first remelting) is given in Table 1. The basic mechanical properties of the alloy are shown in Table 2 in accordance with standard EN 12844.

Table 1. ZnAl4Cu3 alloy chemical composition.

Element Content (wt.%)			
Al	Cu	Mg	Zn
3.93	3.06	0.047	rest
Permissible Elements Content (wt.%)			
Pb	Cd	Sn	Fe
0.0037	0.002	0.0078	0.010

Table 2. Mechanical properties of the ZnAl4Cu3 alloy.

R_m (MPa)		**A_{50} (%)**		**Hardness HBS**	
HPDC	Sand Mold	HPDC	Sand Mold	HPDC	Sand Mold
355	215	5	2	102	90

The casting of test samples was performed with the centrifugal equipment produced by the manufacturer, Atos Bessana (Milano, Italy), consisting of the following:

- Vulcanizer PVM 300 (Figure 1a), in which the vulcanization of the mold takes place at a temperature of 180 °C, under the effect of a pressure 150 bar;
- Melting furnace F50 (Figure 1b) with integrated pyrometer and electronic regulator for setting and maintaining the required melt temperature 420 °C;
- CMRT 300 centrifuge (Figure 1c), which uses centrifugal force to center the silicone mold and fill its cavities with liquid metal.



(**a**) (**b**) (**c**)

Figure 1. Equipment for centrifugal casting: (**a**) vulcanizer, (**b**) melting furnace, and (**c**) centrifuge.

After each cast, a fluidity test, static tensile test, Brinell hardness test, metallographic evaluation, and a fractographic evaluation were performed. The casting of all test specimens was performed with identical conditions, which are listed in Table 3.

Table 3. Casting conditions.

Temperature of the cast metal	$T_k = 420 \pm 5$ °C
Initial temperature of the mold	$T_f = 60 \pm 3$ °C
Rounds per minute of the mold	n = 700 rpm
Solidification time	t = 30 s

The temperature of the cast metal was controlled by the melting furnace pyrometer and the mold temperature by the Digital Checktemp 1 thermometer (Hanna Instruments, Woonsocket, RI, USA), with a 3 mm–diameter puncture probe that was positioned into the pre-drilled hole in the mold.

2.2. Equipment Used and Test Evaluation Methodology

Since fluidity tests for centrifugal casting are not clearly specified, a standard spiral fluidity test was designed and produced (Figure 2). Nine melts were performed, and in each melt six, samples were cast in the clockwise direction of the rotating mold. The batch composition at the first melt consisted of the primary ZnAl4Cu3 alloy. From the P1 melt, the spiral fluidity tests were cast, as well as samples for mechanical tests, metallographic evaluation, and chemical analysis. For the P2 to P9 melts, the composition of the batch material consisted of the remaining material from the previous melt. The number for the letter indicates the number of times the alloy was remelted. Chemical analysis was performed on the P1 alloy (after the first remelting) and on every other alloy (P3, P5, P7, and P9). The results of the chemical analysis are shown in Table 4. The chemical composition was determined by arc spark spectroscopy (Bunker-Q2 ION, Kalkar, Germany).

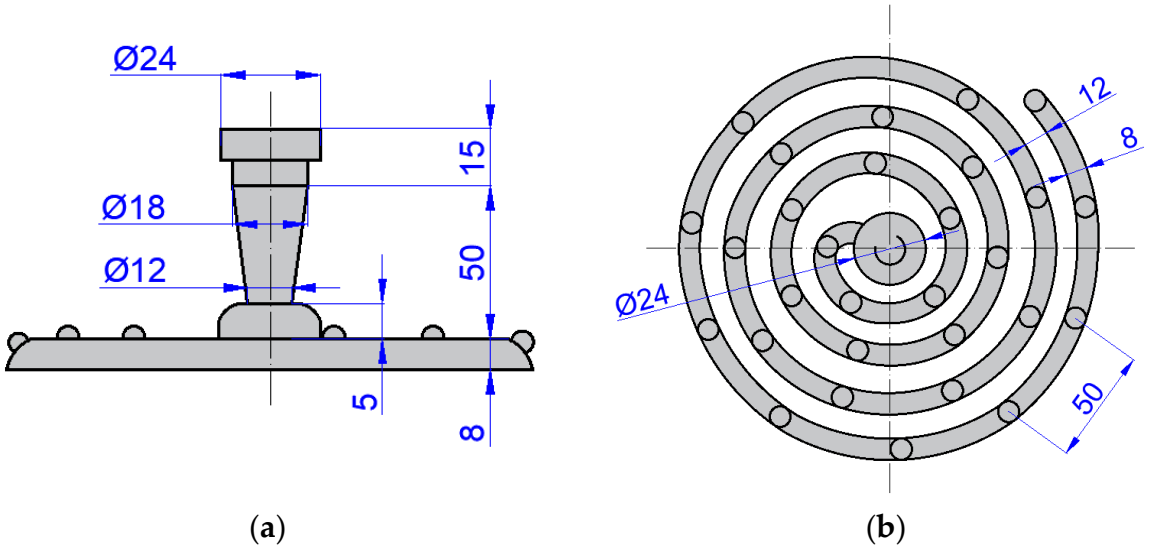


Figure 2. Scheme of spiral fluidity test (dimensions in mm): (**a**) front view and (**b**) top view.

Table 4. Chemical composition of ZnAl4Cu3 alloy depending on the number of remelts.

Alloy	Al (wt.%)	Cu (wt.%)	Mg (wt.%)	Pb (wt.%)	Cd (wt.%)	Sn (wt.%)	Fe (wt.%)	Zn (wt.%)
P3	3.92	2.92	0.040	0.0036	0.002	0.0078	0.011	rest
P5	3.97	2.92	0.042	0.0042	0.002	0.0079	0.012	rest
P7	3.91	2.98	0.039	0.0040	0.002	0.0091	0.011	rest
P9	4.04	2.85	0.045	0.0047	0.003	0.0077	0.0072	rest

The production of all test specimens and spirals from the primary alloy ZnAl4Cu3 with the addition of 3 wt.% Cd was performed under the same conditions as in the previous

case and is labeled by the letter C. A total of nine melts (C1 up to C9) were performed in each, of which six samples were cast. For the C2 to C9 melts, the composition of the batch material consisted of the remaining material from the previous melt. The chemical composition of alloys with Cd addition depending on the number of remelts is given in Table 5.

Table 5. Chemical composition of ZnAl4Cu3 alloy with Cd addition depending on the number of remelts.

Alloy	Al (wt.%)	Cu (wt.%)	Mg (wt.%)	Pb (wt.%)	Cd (wt.%)	Sn (wt.%)	Fe (wt.%)	Zn (wt.%)
C1	3.92	2.42	0.036	0.0047	3.39	0.0096	0.0150	rest
C3	3.84	2.41	0.035	0.0048	3.38	0.0110	0.0078	rest
C5	3.82	2.37	0.035	0.0051	3.50	0.0110	0.0065	rest
C7	3.55	2.54	0.031	0.0046	2.99	0.0120	0.0140	rest
C9	3.76	2.35	0.035	0.0050	3.38	0.0110	0.0078	rest

A static tension test for ZnAl4Cu3 alloy and ZnAl4Cu3 alloy with the addition of 3 wt.% Cd was performed by short cross-section test samples according to standard STN EN 10002-1. The values given are the average of the five measurements.

The measurement was performed according to STN EN ISO 6506-1, under HBS conditions 2.5/187.5/15, on samples taken from the front surfaces of the torn bars from the static tension test. Samples were taken from the first, third, fifth, seventh, and ninth casts. The values given are the average of the five measurements.

Samples for microstructure evaluation were taken from the static tension test bars (1, 3, 5, 7, and 9 casts). The preparation consisted of coarse and fine wet grinding, polishing on an automatic instrument, using diamond emulsion and etching (0.5% HF solution and Dix–Keller for color etching). The microstructure and fracture surfaces of the experimental castings were evaluated by using a NEOPHOT 32 optical microscope and a scanning electron microscope (SEM) with EDX analysis of VEGA LMU II microscope (Tescan, Brno, Czech Republic) coupled to energy dispersive X-ray spectroscopy (Brucker Quantax EDX analyzer, Kalkar, Germany).

3. Results

3.1. Fluidity Evaluation

The average values of the spiral lengths for the individual melts from zinc alloy ZnAl4Cu3 and ZnAl4Cu3 with the addition of 3 wt.% Cd are shown in Figure 3. The spiral length of the ZnAl4Cu3 alloy (without additions) reached the highest value (longest running length 647 mm), as expected for the reference alloy P1 (after the first remelting). After the subsequent remelting, the length of the spiral gradually decreased, and with the P4 alloy, the decrease stabilized at 528 mm, which represents an approximately 18% decrease compared to the reference P1 alloy (Figure 3a).

The experimental alloy ZnAl4Cu3 with a 3% Cd addition reached a high spiral length of 792 mm after the first remelting. The value of the spiral length at the level of about 790 mm was constant even during the subsequent three remeltings. The decrease did not occur until the alloy after the fifth reflow of C5 to 752 mm and continued to a minimum value of 705 mm for the alloy after the ninth reflow of C9 (Figure 3b).

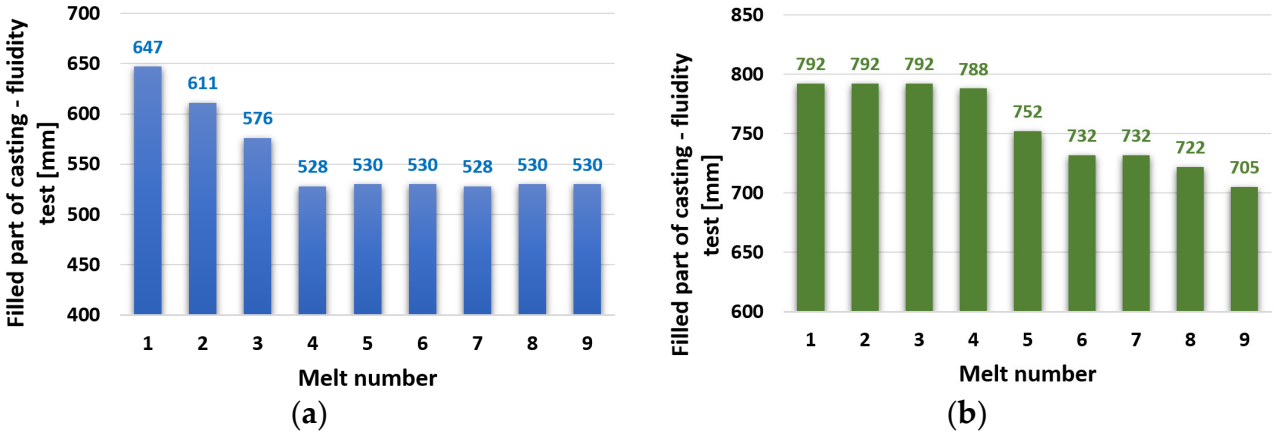


Figure 3. Dependence of spiral fluidity test length on the number of remelts: (**a**) ZnAl4Cu3 and (**b**) ZnAl4Cu3 with 3 wt.% Cd addition.

3.2. Mechanical Properties

3.2.1. Ultimate Tensile Strength (UTS)

The tensile test results are shown in Figure 4. The ZnAl4Cu3 alloy reached a constant value of 272 to 274 MPa after the first five remeltings, and this value also represented the highest tensile strength of the entire spectrum of experimental alloys. The expected decrease occurred after the seventh remelting to the level of UTS = 226 MPa and to the value of UTS = 211 MPa after the ninth remelting. The addition of 3 wt.% Cd to the ZnAl4Cu3 alloy caused a significant decrease in tensile strength. The values ranged from 178 MPa (alloy C3) to 196 MPa (alloy C5).

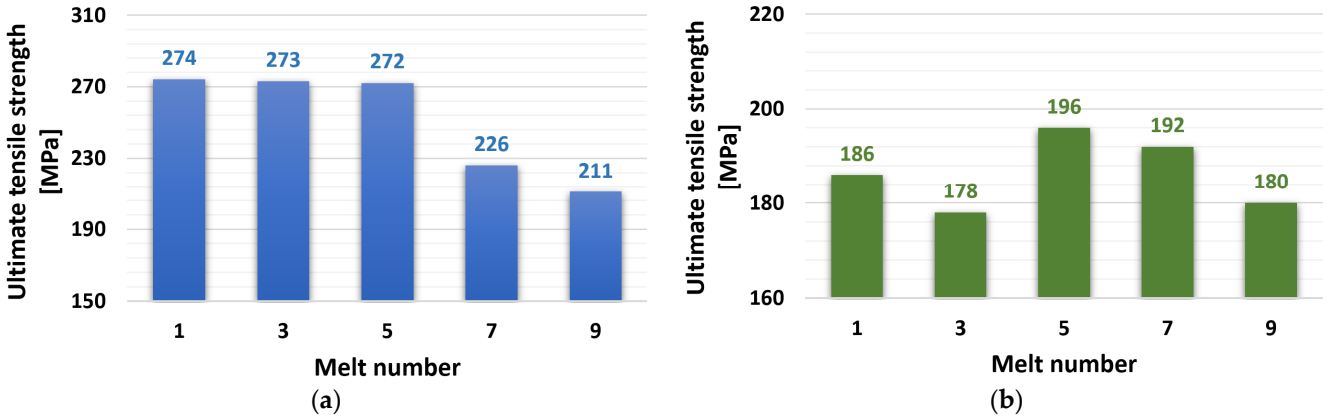


Figure 4. Dependence of ultimate tensile strength on the number of remelts: (**a**) ZnAl4Cu3-P1 to P9 alloys and (**b**) ZnAl4Cu3 with 3 wt.% Cd addition C1 to C9 alloys.

3.2.2. Ductility (A_{50})

The results of ductility test evaluation are shown in Figure 5. The ductility of the ZnAl4Cu3 alloy reached over 2% in all cases. The highest value was measured in the reference alloy, P1, at 2.6%. Alloys of ZnAl4Cu3 with 3 wt.% Cd after the third and seventh remeltings had higher ductility. On the contrary, the lowest ductility in the alloy without the addition of Cd was 2.2%, and with the addition of Cd, it was 1.7%.

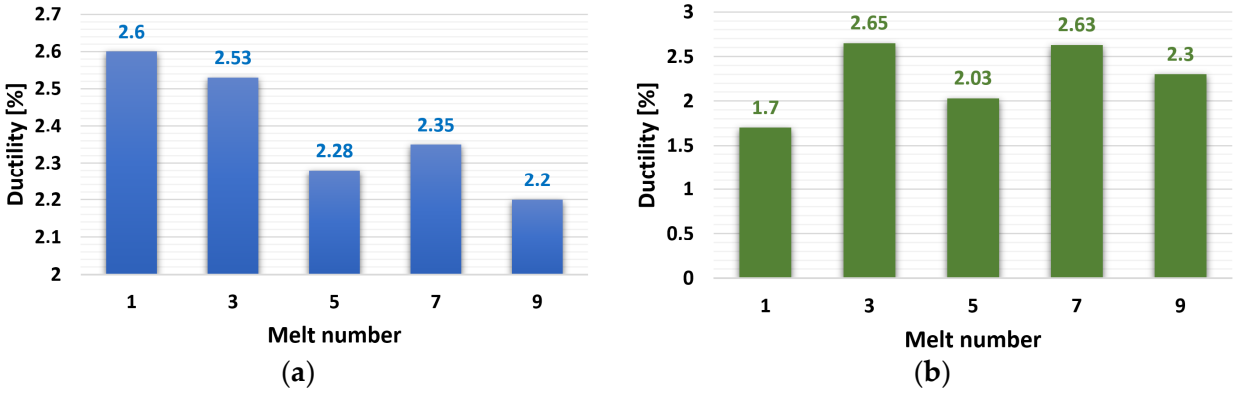


Figure 5. Dependence of ductility on the number of remelts: (**a**) ZnAl4Cu3-P1 to P9 alloys and (**b**) ZnAl4Cu3 with 3 wt.% Cd addition C1 to C9 alloys.

3.2.3. HBW Hardness Evaluation

The measured hardness values are shown in Figure 6, where they are expressed as a dependence of the hardness value on the number of zinc alloy remeltings. The hardness values of the ZnAl4Cu3 alloy had increasing characteristics, from an initial hardness of 128 HBW (reference alloy P1) to 135 HBW (alloy after the fifth remelting), with a subsequent significant decrease to a minimum value of 114 HBW (alloy after the ninth remelting). The hardness values of the ZnAl4Cu3 alloy with Cd addition were kept in a narrow range (116 to 118 HBW).

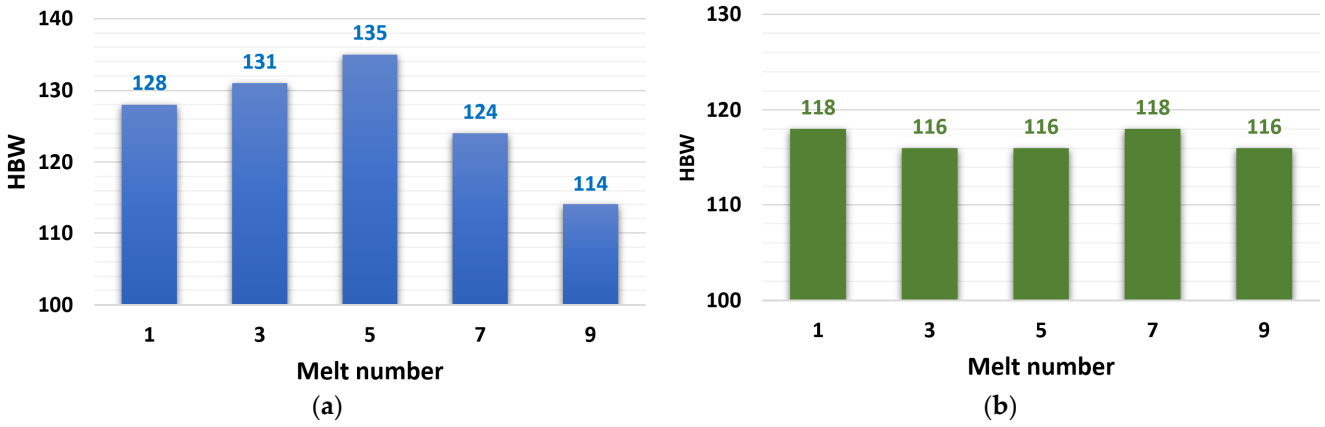
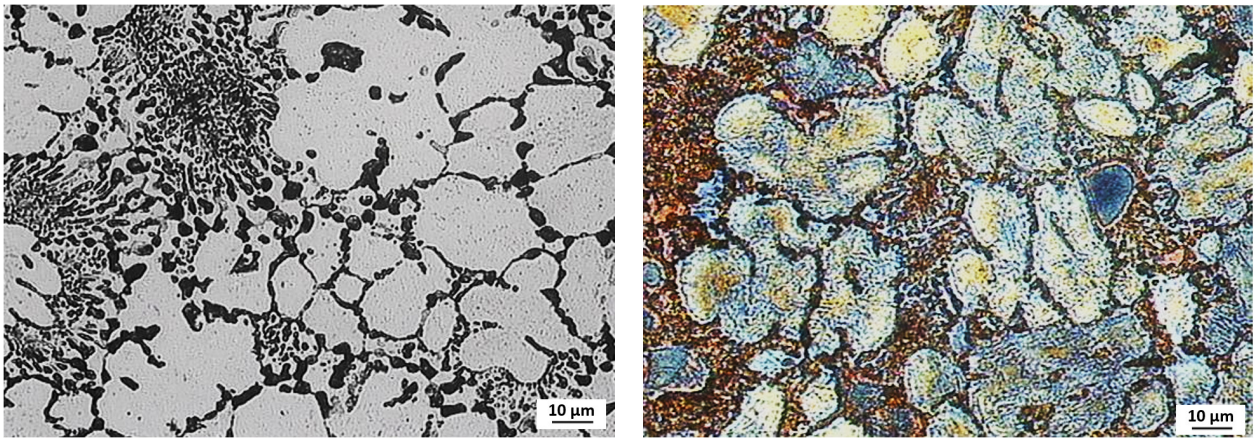


Figure 6. Dependence of ductility on the number of remelts: (**a**) ZnAl4Cu3-P1 to P9 alloys and (**b**) ZnAl4Cu3 with 3 wt.% Cd addition C1 to C9 alloys.

3.3. Evaluation of Microstructure

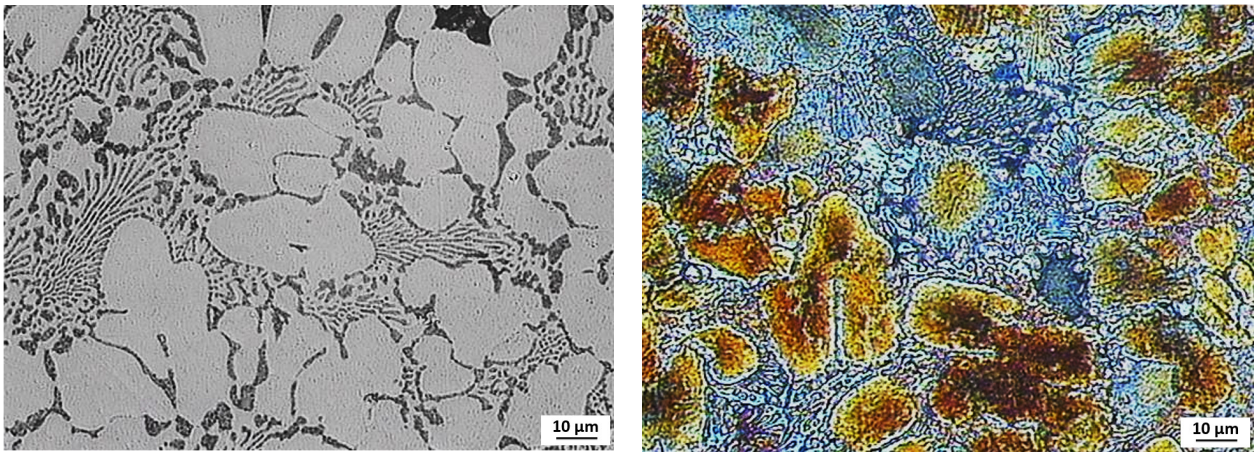
The microstructure of the ZnAl4Cu3 alloy after the first remelting is characterized by the presence of phases η, β, ε, and α (Figure 7). The crystallization process begins with the formation of the η phase (aluminum and copper containing zinc solid solution) and ends with the formation of a eutectic composed of the η and β phases and a eutectic composed of the η, β, and ε phases in the dendritic space.

From the microstructural images of the ZnAl4Cu3 alloy after the fifth (Figure 8) and after the ninth (Figure 9) remelting, an increase in the number of bright spots can be observed in images with etched 0.5% HF, which represent dendrites of η phases. This increase was observed with each subsequent remodeling.



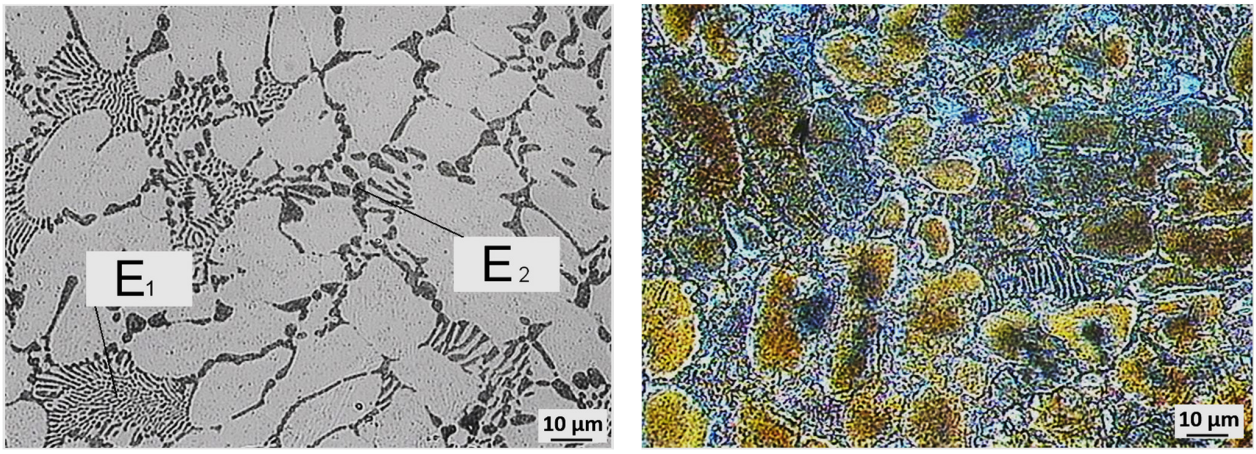
(**a**) (**b**)

Figure 7. Microstructure of the ZnAl4Cu3 sample after first remelting (P1 alloy): (**a**) etched 0.5% HF and (**b**) etched Dix–Keller.



(**a**) (**b**)

Figure 8. Microstructure of the ZnAl4Cu3 sample after fifth melting (P5 alloy): (**a**) etched 0.5% HF and (**b**) etched Dix–Keller.

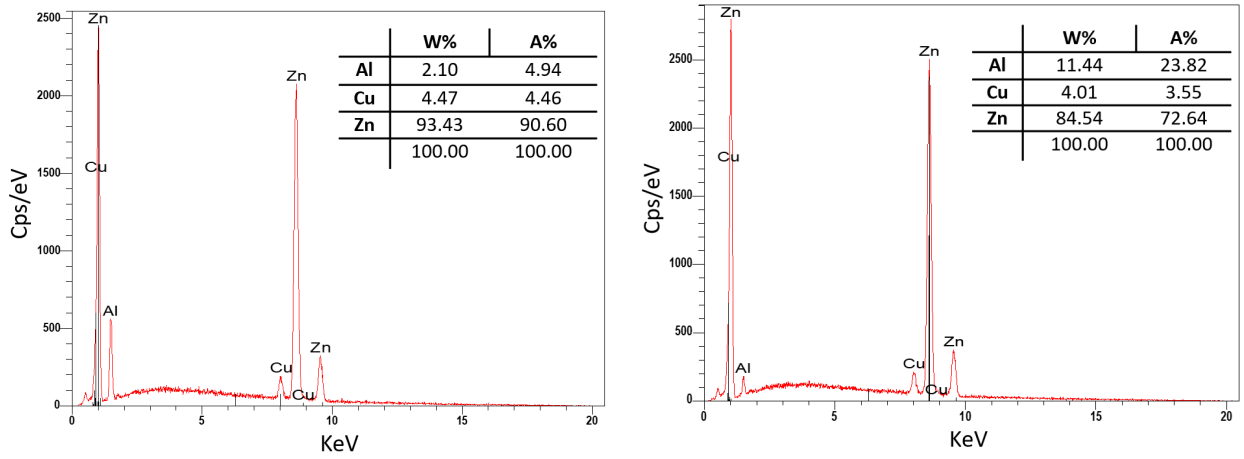


(**a**) (**b**)

Figure 9. Microstructure of the ZnAl4Cu3 sample after ninth melting (P9 alloy): (**a**) etched 0.5% HF and (**b**) etched Dix–Keller.

In the microstructure of the alloy with the highest number of remelting (nine), three morphologically different formations can be observed which form solid solution dendrites, η, and two types of eutectic colonies with different morphology. Eutectic colonies labeled E_1 and E_2 (Figure 9) form lamellar morphological phases and consist of alternately layered lamellae of the α and η phases. The shape and dimensions of the lamellae depend on the cooling rate of the casting. The eutectic decomposition products of the β-phase are coarser (E_2) than the decomposition products of the primary secreted β-phase, which are characterized by a fine vein structure (E_1).

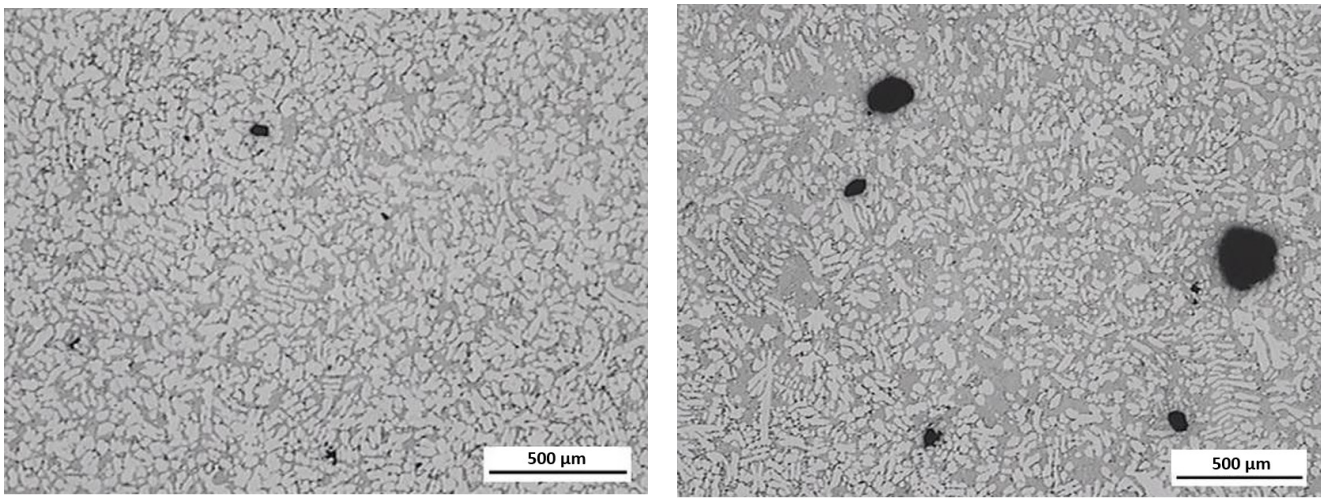
Sample P2 from the second remelting was subjected to a quantitative analysis on a raster electron microscope (SEM), where the composition of the individual phases in the structure was identified. The results of the examined sample are shown in Figure 10. From the analysis of the P2 sample, it can be seen that Zn and Cu are predominantly present in dendrites, and the eutectic is mainly composed of Zn with a higher Al content (11%).



(**a**) (**b**)

Figure 10. Quantitative analysis of P2: (**a**) dendrite-phase $CuZn_4$ and (**b**) eutectics-Al_4Cu_3Zn phase.

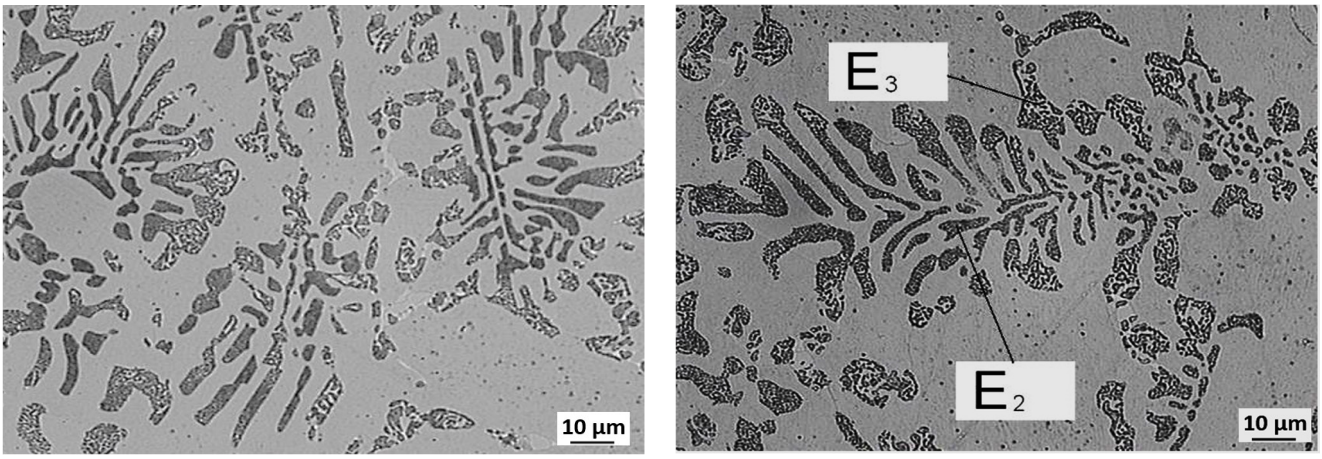
Figure 11 shows a comparison of the structure of the ZnAl4Cu3 alloy after the third and seventh remelts at 25× magnification. The main difference occurred in the presence of pores, their number, and their size.



(**a**) (**b**)

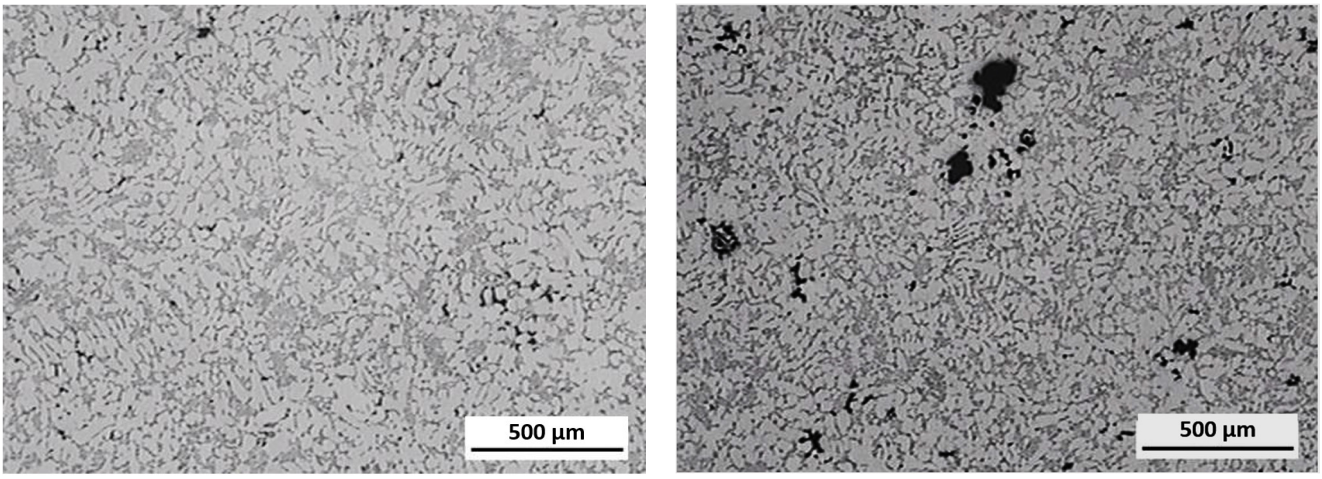
Figure 11. Comparison of the presence of pores in the microstructure of ZnAl4Cu3 alloy: (**a**) after first remelting (P1 alloy) and (**b**) after ninth remelting (P9 alloy).

By adding 3 wt.% Cd to the ZnAl4Cu3 alloy, a quaternary alloy was obtained in which Cd significantly influenced the mechanical properties and morphology of the microstructure (Figures 12 and 13). In the microstructure, we can observe the emergence of a new kind of eutectic, E_3, in the form of glossy surfaces, which are coherent with the eutectic E_2 (Figure 11b).



(**a**) (**b**)

Figure 12. Comparison of ZnAl4Cu3 alloy microstructure with Cd addition, etched 0.5% HF; (**a**) after first remelting (C1 alloy); (**b**) after ninth remelting (C9 alloy).



(**a**) (**b**)

Figure 13. Comparison of the presence of pores in the microstructure of ZnAl4Cu3 alloy: (**a**) after first remelting (C1 alloy) and (**b**) after ninth remelting (C9 alloy).

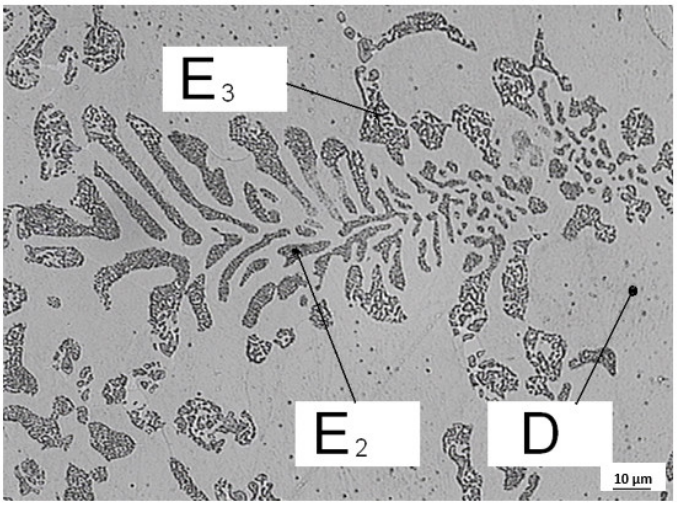
The effect of remelting on ZnAl4Cu3 alloy with Cd addition had an almost identical effect on ZnAl4Cu3 alloy without Cd addition. As the number of remelts increases, the number of bright spots in the images (Figures 12b and 13b), which represent the dendrites of the η phase, increases. This increase was recorded with each subsequent melting. In the microstructure, four morphologically different formations can be observed at a given magnification, which form solid solution dendrites, η, and three types of eutectic colonies with different morphologies. Eutectic colonies designated E_1, E_2, and E_3 have phases with lamellar morphology and consist of alternately layered lamellae of α and η phases. The decay products of the eutectic β phase are coarser (E_2) than the decay products of the primarily precipitated β phase, which are characterized by a fine fan-shaped structure (E_1), which is less present in the microstructure than in the alloy without Cd addition. In the

images at 25× magnification (Figure 13), it can be seen that the porosity in the interdendritic regions increased due to the multiple remeltings.

The C9 sample from the ninth remelting was subjected to quantitative analysis on SEM, where dendrite D and eutectic E_3 were identified. The overall view of the structure is shown in Figure 14, on which the analyzed sites of the structure (D and E_3) are indicated. From the analysis of the C9 sample, it can be seen that Zn and Cu are predominantly present in dendrites D and eutectic E_3 is composed mainly of Zn with a high proportion of Al and Cd.

Dendrite D

	W%	A%
Al	1.45	3.80
Cu	3.93	3.97
Zn	93.31	91.37
Cd	1.51	0.86
	100.00	100.00



Eutectics E3

	W%	A%
Al	21.41	40.26
Cu	2.61	2.08
Zn	71.93	55.83
Cd	4.05	1.83
	100.00	100.00

Figure 14. Microstructure of ZnAl4Cu3 alloy with addition 3 wt.% Cd (C9) with quantitative analysis of eutectic E3 and dendrite D.

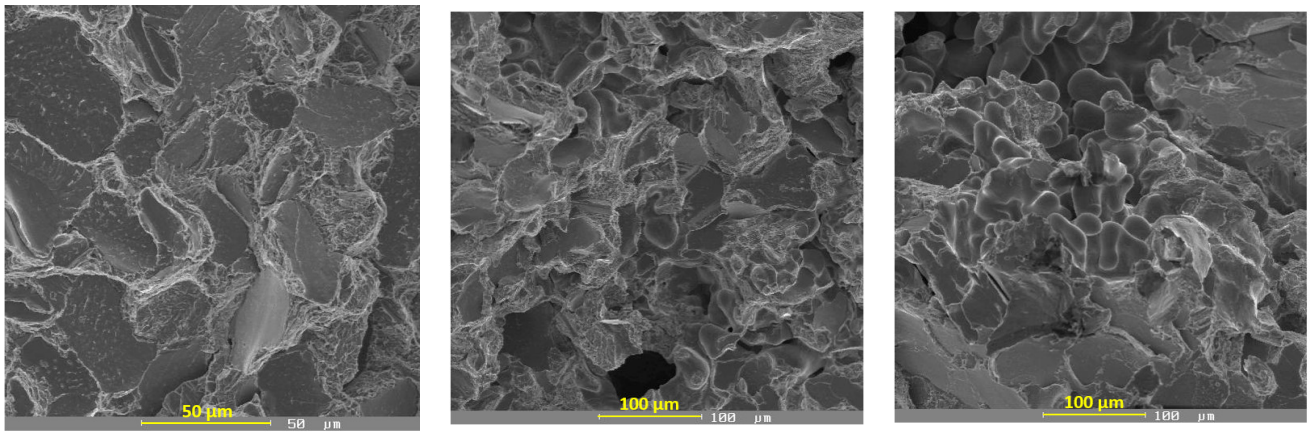
3.4. Fractographic Evaluation

Samples for fracture evaluation were taken from the bars after the tensile test; therefore, all observed areas were subjected to forced static fractures. The facets of the fracture areas on the examined samples exhibit the characteristic morphology of the micro-mechanisms of the intercrystalline breach by ductile scission, where two layers of material were torn apart by plastic deformation during the formation of the fracture surfaces. The fracture area of the sample from the first casting in Figure 15a shows a characteristic "breach" micro-mechanism. The third remelting caused a significant increase of defects on the fracture area (Figure 15b). From Figure 15c, it is evident that nine remeltings had a significant effect on the characteristics of the fracture area. The sample from the ninth remelting is characterized by the greatest number of defects, most of which are cavities of various shapes and sizes, small fragments on the fracture area, and the occurrence of pores.

It can be assumed that casting defects in the form of cavities and pores could arise due to turbulent filling of the mold (reoxidation) and the relatively high rate of heat removal from the casting, or due to endogenous gas exclusion. From the fragment images (Figure 16c), it can be seen that all the fracture areas had the same characteristics, and only the ratio of dark smooth surfaces and ductile light areas is changed.

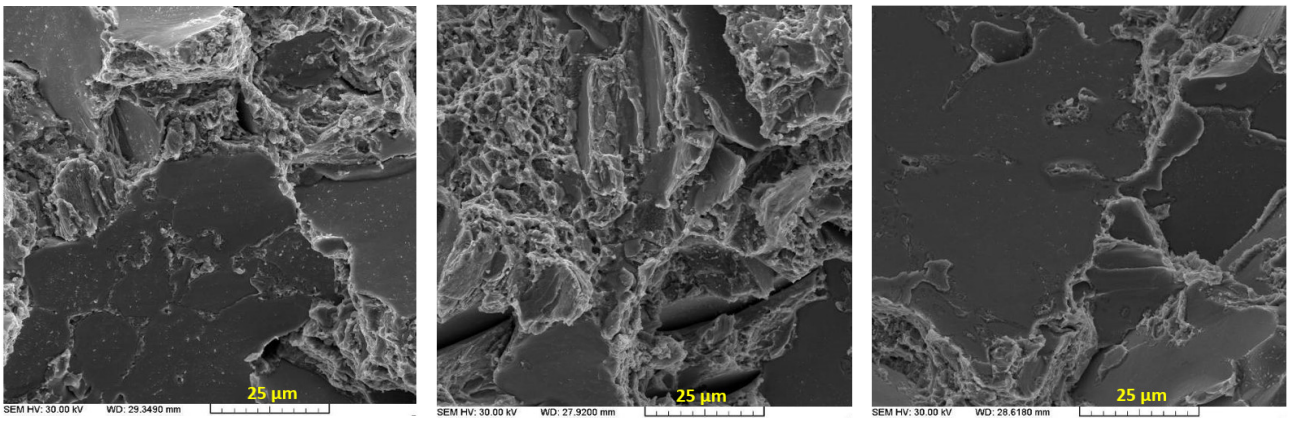
The facets of the fracture areas on the sample from the first melting, C1 (Figure 16a), exhibit the characteristic morphology of the intercrystalline breach micro-mechanisms by ductile scission. From the picture, it can be seen that the representation of the scissible surfaces is larger compared to ductile surfaces. For this sample, the lowest A_{50} was measured. The micro-mechanism of the breach in the sample of the third melting, C3 (Figure 16b), is the same as on the sample of the first melt, but the proportion of the ductile violations increased. This sample showed the highest A_{50} value in the static test. The facets of the fracture areas on the sample from the ninth melt, C9 (Figure 16c), exhibit the characteristic morphology of the intercrystalline breach micro-mechanisms by ductile scission with a small fraction of ductile violations faces and a larger fraction of scission

phases in several planes. This sample showed the smallest UTS values in the static test. From a macroscopic fracture assessment perspective, the fracture area of this sample has the biggest amount of volume defects in the form of cavities and pores of all tested samples from the C1 to C9 melts.



(**a**) (**b**) (**c**)

Figure 15. Fractography evaluation of ZnAl4Cu3 alloy: (**a**) after first remelting, P1; (**b**) after third remelting, P3; and (**c**) after ninth remelting, P9.



(**a**) (**b**) (**c**)

Figure 16. Fractography evaluation of ZnAl4Cu3 alloy with addition 3 wt.% Cd: (**a**) after first remelting, C1; (**b**) after third remelting, C3; and (**c**) after ninth remelting, C9.

4. Discussion

The application of multiple remeltings of the ZnAl4Cu3 alloy led to negative phenomena, which are provable by comparing the microstructure of the alloy after the first and ninth remelting. A decrease of the eutectic in the matrix, coarsening of the grains, and an increase length of the dendritic arms were observed. These negative factors caused a decrease in fluidity with the increasing number of remelts of the experimental ZnAl4Cu3 alloy. The decrease of eutectic in the microstructure of alloys with a higher number of remelts also resulted in an increase of microporosity in the interdendritic regions. The reduction in the proportion of eutectic phases, which is characterized by a higher Al content, together with an increased presence of microporosity, had a decisive influence on the decrease in tensile strength and ductility of alloys with a higher number of remelts [12]. Overall, the largest decrease in tensile strength (23%) was recorded between the first and ninth melts, but a significant difference occurred between the fifth and seventh remelts. Ductility recorded the largest drop between the third and fifth remelting, where it can be

stated that the "deformation" of the structure due to remelting first affected the ductility of the alloy.

The hardness of the ZnAl4Cu3 alloy increased slightly due to remelting until the fifth remelting, which could be due to a change in microstructure (coarsening of grains and growth of dendritic arms), but after seven remeltings, there was a drop to a minimum of 114 HBW. The drop in hardness values was due to the increasing amount of porosity in the alloys after the seventh and ninth remelts.

The addition of 3 wt.% of Cd has a significant impact on technological and mechanical properties. Fluidity values compared to the Cd-free alloy increased by 22.4% from 647 to 792 mm. The reason for this increase is the cadmium's effect on chemical composition and microstructure, as well as on physical properties, in particular, specific heat (232 J kg^{-1} K^{-1}) and latent heat (57.103 J kg^{-1}) [1]. By altering the chemical composition of the alloy, a new phase arose, and it had significant influence on the properties of the alloy. The melting temperature decreased, thereby expanding the melt overheat zone, which is directly proportional to the heat content, which has an impact on the fluidity improvement. Cadmium, among other things, by its low values of specific and latent heat and by higher solid phase density than zinc, improves the meltability of the alloy. Its low surface tension is another factor improving the casting properties. High values of fluidity were preserved also during the ninth remelting, where its value (length of the spiral 705 mm) was still higher than the value of the fluidity of the primary non-cadmium alloy (length of the spiral 647 mm). The effect of remelting on fluidity is negative, because, in all remelted cases, there was a reduction in spiral length.

The addition of cadmium reduced the value of the tensile strength of the alloy, where its highest value measured at the fifth remelting was 196 MPa compared to the primary alloy after the first melting, where the tensile strength was 274 MPa (reduction by 28.5%). This decline occurred by changing the composition of eutectic in the structure.

5. Conclusions

By examining the technological and mechanical properties of the alloy ZnAl4Cu3 during centrifugal casting into the silicone mold, it is possible to recommend up to three-fold remelting of the zinc alloy without any significant reduction of the tensile strength or increase in hardness, and with a slight decrease in ductility. However, the application of the ZnAl4Cu3 alloy remelting led to a decrease in the proportion of eutectic in the matrix and thus to a constant drop of the fluidity values up to the fourth remelting. The microstructure of the ZnAl4Cu3 alloy after the sixth and more remeltings is characterized not only by the reduced proportion of eutectic but also by the coarse-grained structure and larger dimensions of the dendritic arms, which led to a decrease in all observed properties.

The application of 3 wt.% Cd in the ZnAl4Cu3 alloy led to a change in the microstructure by crystallization of the eutectic (morphology of the shiny surfaces in the cut plane with a small proportion of cadmium). The change in microstructure by the addition of cadmium caused an increase of fluidity with a significant decrease in tensile strength. It can be stated that the effect of multiple remeltings of the ZnAl4Cu3 alloy with 3 wt.% cadmium, due to the sudden change of mechanical properties (especially tensile strength and elongation), had no continuous effect. Due to the Rm decrease, using the ZnAl4Cu3 alloy with 3 wt.% Cd is recommended only within a narrow range of products. Its use is important due to its high fluidity, mainly for castings with advanced shapes.

Author Contributions: Conceptualization, D.B. and M.B.; methodology, M.M., D.B. and M.B.; software, M.M.; validation, D.B. and M.B.; formal analysis, M.M. and D.B.; investigation, M.M. and M.B.; resources, D.B. and M.B.; data curation, M.B. and M.M.; writing—original draft preparation, D.B. and M.M.; writing—review and editing, D.B., M.B. and M.M.; visualization, M.B. and M.M.; supervision, D.B.; project administration, D.B.; funding acquisition, D.B. and M.B. All authors have read and agreed to the published version of the manuscript.

Funding: The article was created as part of the VEGA grant agency project: VEGA 1/0160/22. The authors thank the agency for its support.

Institutional Review Board Statement: Not applicable.

Informed Consent Statement: Not applicable.

Data Availability Statement: Data available upon request. The data presented in this study are available upon request from the corresponding author.

Conflicts of Interest: The authors declare no conflict of interest.

References

1. Shurkin, P.; Belov, N.; Akopyan, T.; Karpova, Z. Recycling-oriented design of the Al-Zn-Mg-Ca alloys. *Mater. Proc.* **2021**, *3*, 7. [CrossRef]
2. Tan, R.; Khoo, H. Zinc Casting and Recycling. *Int. J. Life Cycle Assess* **2005**, *10*, 211–218. [CrossRef]
3. Westing, E.; Savran, V.; Hofman, J. *Recycling of Metals from Coatings*; Materials Innovation Institute M2i: Delft, The Netherlands, 2013.
4. Lynch, R.F. Zinc: Alloying, Thermomechanical Processing, Properties, and Applications. In *Encyclopedia of Materials: Science and Technology*; Elsevier: Amsterdam, The Netherlands, 2001; pp. 9869–9883.
5. Dudek, P.; Piwowońska, J. Influence of Titanium on the Microstructure and Mechanical Properties of Foundry Zinc Alloy. *J. Mater. Eng. Perform.* **2022**. [CrossRef]
6. Kaya, M.; Hussaini, S.; Kursunoğlu, S. Critical review on secondary zinc resources and their recycling technologies. *Hydrometallurgy* **2020**, *195*, 105362. [CrossRef]
7. Lu, X.; Miki, T.; Sasaki, Y.; Nagasaka, T. Thermodynamic criteria of alloying elements elimination during recycling end-of-life zinc-based products by remelting. Resources. *Conserv. Recycl.* **2022**, *176*, 105913. [CrossRef]
8. Rollez, D.; Pola, A.; Prenger, F. Zinc alloy family for foundry purposes. *World Metall.* **2015**, *68*, 354–358.
9. SM International Committee. *Properties and Selection: NonferrousAlloys and Special Purpose Materials, ASM Metals Handbook*, 10th ed.; ASM International: Almere, The Netherlands, 1990; Volume 2, p. 1300.
10. Li, B.J.; Chao, C.G. Aging Kinetics of Heat-Treated Zn–4Al–3CuAlloy. *Scr. Mater.* **1999**, *41*, 143–147. [CrossRef]
11. da Silva, F.C.; Kazmierczak, K.; da Costa, C.E.; Milan, J.C.G.; Torralba, J.M. Zamak 2 Alloy Produced by Mechanical Alloying and Consolidated by Sintering and Hot Pressing. *J. Manuf. Sci. Eng.* **2017**, *139*, 091011. [CrossRef]
12. Haynes, W.M. *CRC Handbook of Chemistry and Physics*, 96th ed.; CRC Press: Boca Raton, FL, USA; Taylor & Francis: Oxfordshire, UK, 2015; pp. 243–247.
13. Al-Maharbi, M.; Karaman, I.; Purcek, G. Flow response of a severe plastically deformed two-phase zinc–aluminum alloy. *Mater. Sci. Eng. A* **2010**, *527*, 518–525. [CrossRef]
14. Pürçek, G. Improvement of mechanical properties for Zn–Al alloys using equal-channel angular pressing. *J. Mater. Process. Technol.* **2005**, *169*, 242–248. [CrossRef]
15. Purcek, G.; Altan, B.S.; Miskioglu, I.; Ooi, P.H. Processing of eutectic Zn–5% Al alloy by equal-channel angular pressing. *J. Mater. Process. Technol.* **2004**, *148*, 279–287. [CrossRef]
16. da Costa, E.M.; da Costa, C.E.; Vecchia, F.D.; Rick, C.; Scherer, M.; dos Santos, C.A.; Dedavid, B.A. Study of the Influence of Copper andMagnesium Additions on the Microstructure Formation of Zn–Al HypoeutecticAlloys. *J. Alloys Compd.* **2009**, *488*, 89–99. [CrossRef]
17. Wu, Z.; Sandlöbes, S.; Wu, L.; Hu, W.; Gottstein, G.; Korte-Kerzel, S. Mechanical behaviour of Zn–Al–Cu–Mg alloys: Deformation mechanisms of as-cast microstructures. *Mater. Sci. Eng. A* **2016**, *651*, 675–687. [CrossRef]
18. Lakomá, R.; Čamek, L.; Lichý, P.; Kroupová, I.; Radovský, F.; Obzina, T. Some Possibilities of Using Statistical Methods While Solving Poor Quality Production. *Arch. Foundry Eng.* **2021**, *21*, 18–22.
19. LeHuy, H.; L'Espérance, G. Ageing characteristics of dendritic and non-dendritic (stir-cast) Zn-Al alloy (ZA-27). *J. Mater. Sci.* **1991**, *26*, 559–568. [CrossRef]
20. Pola, A.; Tocci, M.; Goodwin, F.E. Review of Microstructures and Properties of Zinc Alloys. *Metals* **2020**, *10*, 253. [CrossRef]